Transport of Passive Scalars in Neutrally and Stably Stratified Homogeneous Turbulent Shear Flows

H.-J. Kaltenbach, T. Gerz and U. Schumann

DLR, Institut für Physik der Atmosphäre, W-8031 Oberpfaffenhofen
Germany

The dispersion of a passive scalar in a turbulent flow can be described by the turbulent diffusivity tensor D_{ij} which relates the turbulent flux of a scalar fluctuation c to the gradient of its mean value C according to $\overline{u_i c} = -D_{ij}\partial C/\partial x_j$. By means of Direct Numerical Simulation we show how components of the unsymmetric tensor behave under the influence of shear and thermally stable stratification. From an analysis of three-dimensional flux spectra it turns out that weakly stratified flows are dominated by large scale motions. The total fluxes can then sufficiently be explained by linear theory like RDT. However, in moderatly stratified flows we find significant small-scale contributions with signs opposing to the large scales. These are due to non-linearity and should be considered in scalar dispersion models.

1. Introduction and method

We extend the study of Rogers, Mansour & Reynolds (1989), who calculated the development in time of the components of D_{ij} for an unbounded shear flow, to stably stratified flows. They derived an algebraic flux model which predicts D_{ij} from the Reynolds stresses and the mean strain-rate.

Our Direct Numerical Simulation captures all relevant scales of a turbulent flow at low Reynolds number. The time-dependent, three-dimensional Navier-Stokes equations in the Boussinesq approximation for the velocity fluctuations u, v and w and the balances of the temperature fluctuation T and of three passive scalar fluctuations c_1 , c_2 and c_3 are integrated in space and time. Figure 1 shows the computational domain and profiles

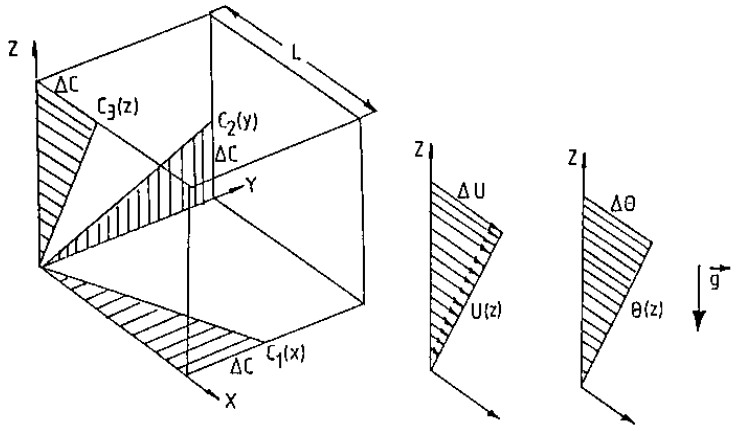

Figure 1. The computational domain is a cubus with axes x, y and z. Note the uniform gradients of the mean quantities U, Θ, C_1, C_2 and C_3

Advances in Turbulence 3
Editors: A.V. Johansson · P.H. Alfredsson

of the mean quantities. Velocity U and temperature Θ have uniform vertical gradients S and s. whereas the mean scalar fields C_1, C_2, C_3 possess gradients s_1, s_2, s_3 in the streamwise (x-), spanwise (y-) and vertical (z-) direction, respectively. Temperature fluctuation T and scalar fluctuation c_3 behave identically because we consider only cases with equal molecular diffusivities ($Pr = Sc$).

The horizontal boundaries are periodical, the vertical is shear-periodic. Our code uses central differences, an explicit integration scheme in time (Adams-Bashforth) and a pseudospectral approximation of the advection by the mean flow. The grid resolution is 128 cells in each direction. For details see Gerz, Schumann & Elgobashi (1989).

Firstly, we performed a simulation under neutral stratification (temperature with vertical gradient as passive scalar) starting from an isotropic velocity field with a given energy spectrum. When this flow has reached self-similar behaviour with characteristic properties of a developed shear flow, we then take these data as initial fields for runs labeled as A to D in Table 1.

Table 1. Nondimensional parameters of developed shear flow at the onset of buoyancy forces at shear time $St = 6$. Results from wind tunnel experiments carried out by Tavoularis & Karnik (1989) with Re_λ between 120 and 400 are given in brackets.

Box length, integral length	$L/L, \ell/L$		1, 0.09	
Taylor micro-l., Kolmogorov l.	$\lambda_{11,1}/L$, l_K/L		0.084, 0.004	
rms of velocity	$v' = (\overline{u_i u_i}/3)^{1/2} = (2E_{kin})^{1/2}$		0.025	
rms of temperature	$T' = (\overline{TT})^{1/2} (= c_3')$		0.049	
rms of concentration	$c_1' = (\overline{c_1 c_1})^{1/2}, c_2'$		0.099, 0.067	
Shear number	$Sh = (\Delta U/L)(\ell/v')$		3.2	
Reynolds number	$Re_\lambda = v'\lambda_{11,1}/\nu$		64	
Prandtl, Schmidt number	Pr, Sc		1, 1	
Reynolds stresses	$\overline{u^2}/(2E_{kin}), \overline{v^2}/(2E_{kin})$		0.56 (0.51),0.29(0.27)	
	$\overline{w^2}/(2E_{kin}), \overline{uw}/(2E_{kin})$		0.15(0.22),-0.16(-0.16)	
Richardson number for case	A	B	C	D
$Ri = \alpha g(\Delta\Theta/L)/(\Delta U/L)^2$	0	0.16	0.33	0.66

2. Results

2.1 Development of kinetic energy and turbulence variances

The shear number $Sh = (\Delta U/L)(\ell/v')$ approximately measures the ratio of energy production by shear and destruction by dissipation ϵ. For $Sh = 3.2$ the kinetic energy grows in the neutral case. The balances of the kinetic energy $\partial E_{kin}/\partial t = -S\overline{uw} + Ri\overline{wT} - \epsilon$ and the potential energy $\partial E_{pot}/\partial t = -Ri\overline{wT} - 0.5Ri\epsilon_{TT}$ reveal the role of the vertical heat flux $\overline{w}T$. It transfers energy from its kinetic form $E_{kin} = 0.5(v')^2$ into the potential form $E_{pot} = 0.5Ri(T')^2$. Depending on the strength of stability, the kinetic energy grows or decays according to an exponential law (Figure 2a). Due to the low Reynolds number of the flow, the critical Richardson number, at which the flow reaches steady state, has a value of 0.16, which is smaller than the typical value of 0.25 for inviscid linear cases as discussed by Gerz & Schumann (1990).

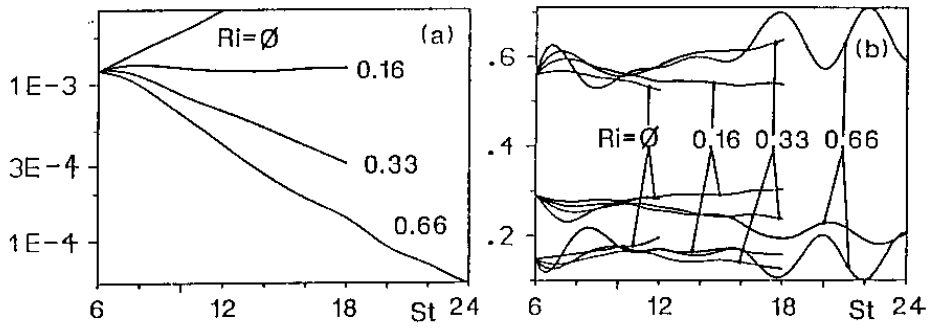

Figure 2. (a) Logarithmic plot of the kinetic energy versus shear time St. (b) Components of the Reynolds stress tensor versus St. Upper, middle and lower curves correspond to $\overline{uu}/(2E_{kin})$, $\overline{vv}/(2E_{kin})$ and $\overline{ww}/(2E_{kin})$, respectively.

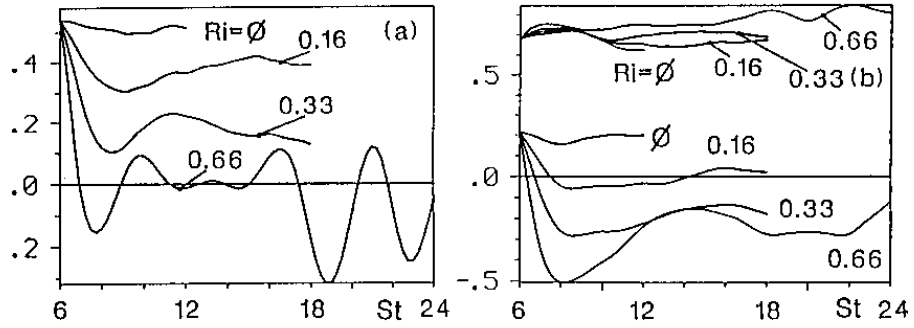

Figure 3. Correlation coefficients of the vertical momentum flux $-\overline{uw}/u'w'$. (a) and the scalar fluxes $\overline{uT}/u'T'$ (upper values) and $\overline{wc_1}/w'c_1$ (lower values) (b) versus time St.

The strong anisotropy of the flow is not much changed by the stratification (Figure 2b). Except for the strongly stable case D, all cases show steady normalized variances; i.e. the flow is self-similar. The anisotropy extends over all scales of the velocities because of the considerable viscosity of the flow. With increasing stability the vertical momentum flux vanishes (Figure 3a) because vertical motions which cause temperature fluctuations are damped by buoyancy forces. Oscillations with twice the Brunt-Väisälä frequency $N = S\sqrt{Ri}$ result from the linear forcing terms by shear and buoyancy.

2.2 Scalar fluxes and diffusivity tensor

The three fluxes $\overline{uc_j}$, $\overline{vc_j}$, $\overline{wc_j}$ of each of the three scalars c_1, c_2, c_3 divided by the mean gradients $-dC_j/dx_j = -s_j$ form the nine components of the turbulent diffusivity tensor $D_{ij} = -\overline{u_i c_j}/s_j$. Due to normalization, $s_j = 1$ and therefore $D_{ij} = -\overline{u_i c_j}$. In our case D_{12}, D_{21}, D_{23} and D_{32} are zero because of flow symmetry. The diagonal components D_{11}, D_{22} and D_{33} describe down-gradient transport along the axes whereas $D_{13} = -\overline{uc_3} = -\overline{uT}$ and $D_{31} = -\overline{wc_1}$ express fluxes orthogonal to the mean gradients which cause them. The velocity variances times the mean scalar gradients s_i form the production terms in the scalar flux balances (1a, 1c and 1e; Φ denotes pressure terms, ϵ denotes molecular smearing). Their anisotropy gives rise to the strong anisotropy of the diffusivity tensor. D_{31} and D_{13} both contain the momentum flux or shear stress

$\overline{uw}$ in the production term (1b and 1d). The additional term $\overline{wT}S$ in the $\overline{uT}$-balance causes the asymmetry of the diffusivity tensor in the neutral case. $Ri\overline{Tc_1}$ enhances the asymmetry for cases with $Ri > 0$.

$$D_{11}: \quad \frac{\partial \overline{wc_1}}{\partial t} = -\overline{uu}s_1 - \overline{wc_1}S + \phi_{1c_1} - \epsilon_{1c_1} \tag{1a}$$

$$D_{31}: \quad \frac{\partial \overline{wc_1}}{\partial t} = -\overline{uw}s_1 + Ri\overline{Tc_1} + \phi_{3c_1} - \epsilon_{3c_1} \tag{1b}$$

$$D_{22}: \quad \frac{\partial \overline{vc_2}}{\partial t} = -\overline{vv}s_2 + \phi_{2c_2} - \epsilon_{2c_2} \tag{1c}$$

$$D_{13}: \quad \frac{\partial \overline{uT}}{\partial t} = -\overline{uw}s - \overline{wT}S + \phi_{1T} - \epsilon_{1T} \tag{1d}$$

$$D_{33}: \quad \frac{\partial \overline{wT}}{\partial t} = -\overline{ww}s + Ri\overline{TT} + \phi_{3T} - \epsilon_{3T} \tag{1e}$$

Because of the tensor asymmetry there is no analogy between turbulent and molecular diffusivity (e.g. heat conduction in an anisotropic medium) which is always symmetric according to the Onsager-Casimir theorem.

The time series of the scalar flux correlation coefficients become more or less stationary as to be expected in a self-similar flow (Figure 3b). If the turbulent diffusivity is an universal property of the flow, the ratios of the scalar fluxes should become steady. Other than Rogers et al. (1989) we use the spanwise flux (or D_{22}) in order to normalize the other fluxes because the vertical scalar (heat) flux reaches very small values in strongly stable cases (Figure 4a). Although these time series do not show exact steady state, they give us some approximate values of the normalized tensor components as a function of Ri (Figure 4b). For D_{13} and D_{33} measured values are available in the neutral case. As Rogers et al. (1989) pointed out, it is practically impossible to realize a stationary mean scalar gradient in the streamwise direction in a laboratory experiment.

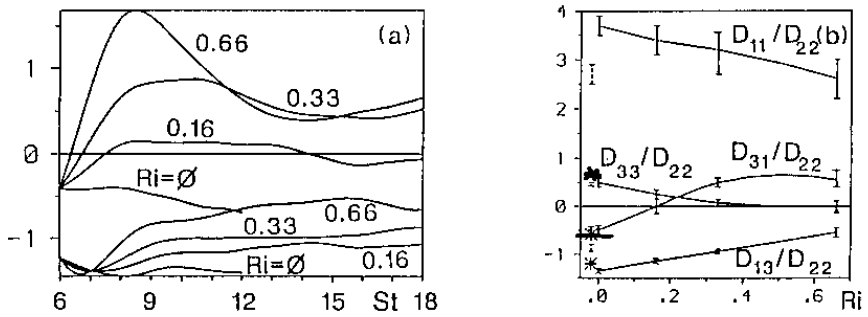

Figure 4. (a) Components of the diffusivity tensor, normalized by the spanwise component D_{22} versus time St; upper values correspond to D_{31}/D_{22}, lower values to D_{13}/D_{22} (b) Normalized diffusivity tensor versus Richardson number at $St > 12$. The dashed error bars mark values from Direct Numerical Simulations of Rogers et al. (1989). Stars mark measured tensor components from Tavoularis & Corrsin (1981 and 1985).

The stability has significant influence on the tensor components D_{33} and D_{31}, both of them expressing vertical fluxes. The sign change of D_{31} results from the fact that the production term $-\overline{uw}s_1$ is counterbalanced by the sink $Ri\overline{Tc_1}$ (1b). The large correlation of the scalar fluctuations T' and c_1 extends over all scales and is not much affected by the stability, except for case D. Explanation of scalar flux behaviour is limited to simple qualitative statements if only the balances (1a-1e) are used. However, Hunt, Stretch & Britter (1988) showed, that important aspects of the flow behaviour are derivable using linear RDT. From a detailed discussion of the distribution of flux contributions on several scales - which is done in the next section - it turns out that some of the scalar fluxes show opposing contributions on large and small scales which are due to non-linearity.

2.3 Spectral analysis of flux behaviour for neutral stratification

In order to understand how the flow is affected by the buoyancy forces it is useful to discuss the neutral flow first. We extend Rogers et al.'s work by analysing the three-dimensional flux spectra of momentum and scalars of our neutral case A, which is comparable to their flow cases. Results from Brasseur & Lin (1990) who analysed the data of Rogers' simulations, are very useful to interprete the spectra. By means of a sampling method they looked out for spots with strong local momentum flux uw which they called "events". They found that the most intense uw-events are completely dominated by negative uw-fluctuations - which can be expected from mixing-length theory - whereas weak events cause as often negative as positive uw-fluxes. In our simulation we find positive uw at 33 % of all grid points and a value of 2.7 for the ratio of rms-values of negative and positive uw-samples, which is consistent with the results of Brasseur.

The shear-stress spectrum Φ_{uw} has strong negative contributions at large scales (see Figure 5a). We find a sharp decrease at medium wave numbers and almost no contributions at small scales. Analysis of the isocontour plot of uw illuminates that the low wave-number contributions mark rather the distance between strong negative events than their spatial extension. The absence of small-scale contributions in Φ_{uw} does not say that there is no small-scale momentum flux. It expresses rather the fact

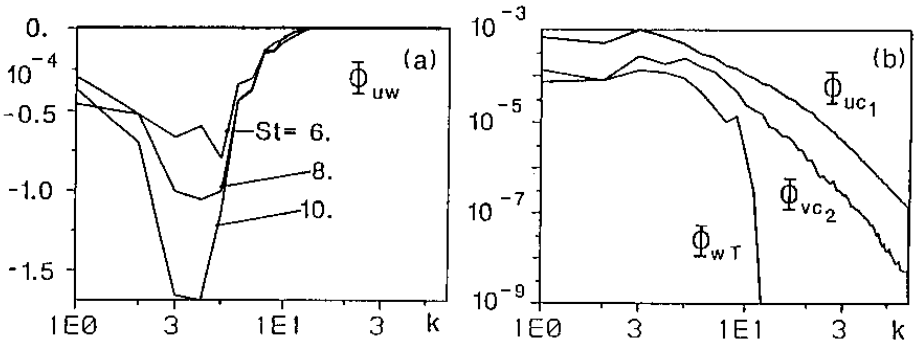

Figure 5. Cospectra versus wave number k of the momentum flux Φ_{uw} (a) at several times and of $-\Phi_{uc_1}$, $-\Phi_{vc_2}$ and $-\Phi_{wT}$ (b) at $St = 9$. The countergradient values (originally positive) of Φ_{wT} are omitted due to the logarithmic axis. Wave-number $k = 1$ corresponds to a wave-length L.

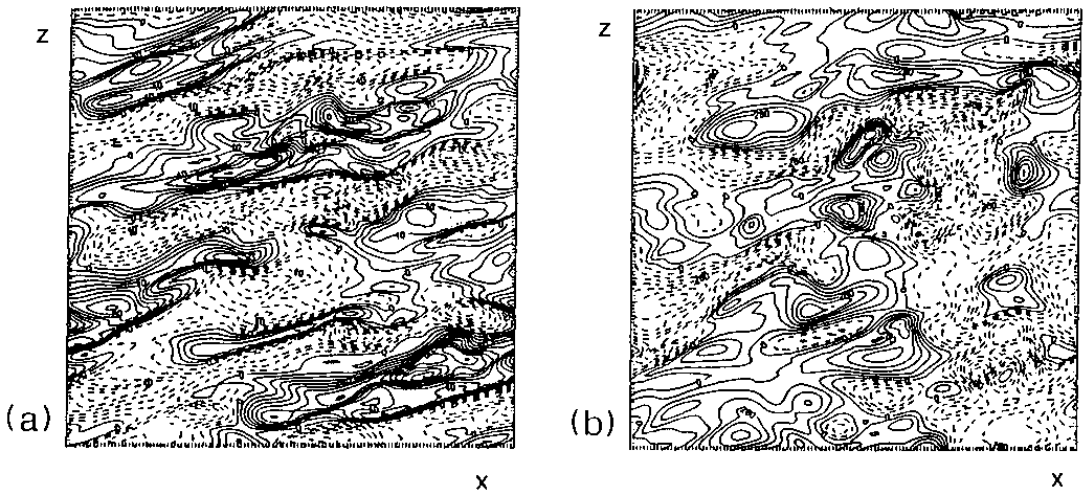

Figure 6. Isocontours of velocitiy fields of u (a) and w (b) from case A with $Ri = 0$ in a x-z plane at $St = 6$.

that at small scales the positive and therefore counter-gradient shear-stress is as big as the negative one. Vanishing shear-stress on small scales, however, does not indicate local isotropy in our case, since we observe an anisotropic flow behaviour at **all** scales. Further, in case of local isotropy, there would be no cause for the strikingly different shapes of the cospectra of the down-gradient scalar fluxes shown in Figure 5b. Since the three scalars c_1, c_2 and $c_3 = T$ differ only with regard to the orientation of their mean gradients, one would expect, that the cospectra look similar at high wave numbers in an locally isotropic flow.

The vertical velocity fluctuation w behaves differently than horizontal fluctuations u and v. Comparison of vertical cross-sections of the fields of u and w (Figure 6) gives rise to the conjecture that the w-fluctuations play the key-role in this flow, since the w-field looks more random and, hence, changes sign more frequently, whereas the u-fluctuations show some inclined streaky coherent structures (see also Gerz, 1990). This is consistent with the fact that the skewness-coefficients of the velocity derivatives show strong skewness of vertical and horizontal derivatives of u but only weak values of the corresponding coefficients of w. The physical reason for this behaviour is the orientation of the gradient of the mean velocity $U(z)$.

Thus, if we accept the key-role of w-fluctuations, we are able to present a concept of the evolution of a probable flow event. Strong events which caused negative uw and other scalar fluxes according to mixing-length theory break down into small-scale fluid parcels which carry their properties for some time, e.g. horizontal velocity fluctuation u and scalar properties like T and c_1. If w changes sign before the fluid parcels have lost their properties from the past event, vertical fluxes uw and wT will become counter-gradient. Also wc_1 will change sign. On the other hand, small-scale fluxes or correlations which do not involve vertical motion, e.g. uT, uc_1 and c_1T will retain the same values as in the event. In Figure 7 it is tried to sketch the evolution of a "typical" event.

The figure illustrates how properties of a fluid parcel, which starts with mean values of its surroundings according to its initial position, change during a vertical upward displacement $\Delta z(t)$ which is followed by a break-up into several small-scale fluid parcels under the action of turbulence. Some of the small-scale "relics" - still

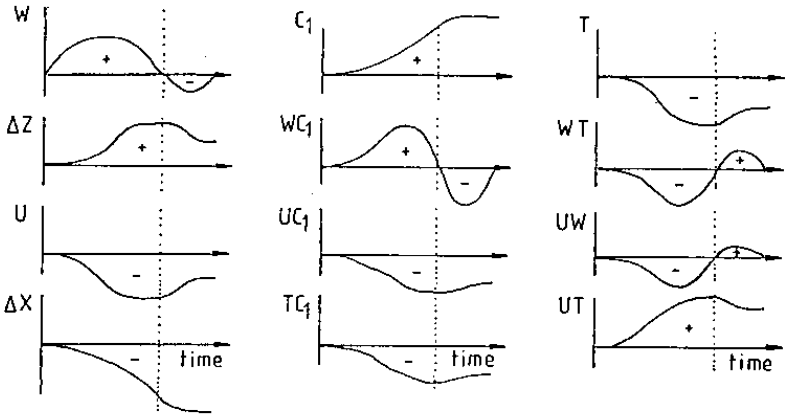

Figure 7. Sketch of properties of a fluid parcel versus time during a "typical" flow event. The dotted lines mark the time when the fluid parcel breaks up into small-scale parcels.

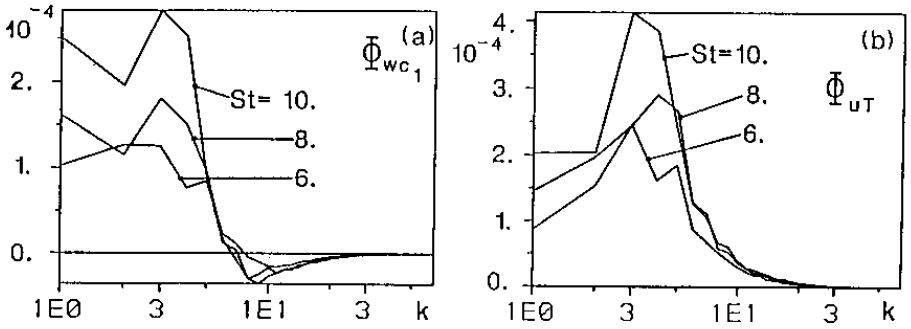

Figure 8. Cospectra from case A with $Ri = 0$ at several times of Φ_{wc_1} (a) and of the streamwise heat flux Φ_{uT} (b).

carrying some of their initial properties - undergo a sort of "compensating" downward motion. It is possible to derive all other fluctuations from the development of w, if one uses the relations $w = d(\Delta z)/dt$, $u = d(\Delta x)/dt \approx -\Delta z dU/dz$, $T \approx -\Delta z d\Theta/dz$, $c_1 \approx -\Delta x dC_1/dx$, where Δx only considers the horizontal displacement caused by the fluctuation u. This presentation is consistent with the moving reference frame due to the mean advection $U(z)$.

So we can subdivide the correlations into two groups. The fluxes uw, wT and wc_1 change their sign during the break-down of the event whereas uT, uc_1 and c_1T retain their signs. It turns out that the cospectra of these correlations can be separated into the same two classes. Cospectra Φ_{uT}, Φ_{uc_1} and Φ_{c_1T} have similar shapes and do not change sign (Figure 8b) whereas Φ_{uw}, Φ_{wT} and Φ_{wc_1} show sharp decreases at medium wave numbers followed by opposing or vanishing contributions at small scales (Figure 8a).

Whereas Φ_{wT} has small-scale counter-gradient contributions (not shown here) Φ_{uw} does not (Figure 5). This can be explained by the longer life time of scalar fluctuations T than of velocity fluctuations u for $Pr \approx 1$. The negative small-scale parts in Φ_{wc_1} have two causes. Firstly, due to ${c_1}'/T' \approx 2$, the flux wc_1 is greater than wT on average; $(wc_1)' \approx 2(wT)'$. Secondly, the different orientation of the mean gradients of u and T on one side and of c_1 on the other side leads to the distinct small-scale behaviour. From the sketch of an event (Figure 7) it is evident that a vertical backward motion

reduces the values of T and u whereas it does not affect c_1. Therefore wc_1 stays relatively large on small scales. The shape of the cospectrum Φ_{wc_1} emphasizes that non-linear effects can have considerable contributions. The subdivision into two groups also holds if one regards the correlation coefficients. The first group with $\overline{uw}/u'w' = -0.5$, $\overline{wT}/w'T' = -0.4$ and $\overline{wc_1}/w'c_1' = 0.2$ has smaller values than the second group with $\overline{uc_1}/u'c_1' = -0.75$, $\overline{uT}/u'T' = 0.65$ and $\overline{c_1T}/c_1'T' = -0.75$.

2.4 Buoyancy influence on the spectra

The moderately stratified cases B and C show similar shape of spectra as the neutral case. However the large-scale contributions are smaller, the high wave-number parts of Φ_{uw}, Φ_{wT} and Φ_{wc_1} are distinctly counter-gradient (not shown here). We conclude that buoyancy acts on **all** scales of a shear flow at the given (small) Reynolds number. The large-scale upward motion in our flow example (Figure 7) is diminished by the stratification, whereas the small-scale "compensating" downward displacement is enhanced due to the body force which draws the fluid-parcels with negative T-fluctuation downwards. T and c_1 stay strongly correlated in stratified flows except for case D which indicates that the mechanism of flow events given above is adequate even for the description of moderately stratified flows. From the distinct opposing behaviour at different scales we conclude that accurate modeling of scalar dispersion under stable stratification will be difficult.

References

Brasseur, J.G. & Lin, W.-Q. 1990 Structural and statistical characteristics of intermittency in homogeneous turbulent shear flow. In: *Proc. Third European turbulence conference*, Stockholm 1990.

Gerz, T. 1990 Coherent structures in stratified turbulent shear flows deduced from direct simulations. In: *Turbulence and Coherent Structures.* (M. Lesieur & O. Metais, eds.), Kluwer Academic Publishers, in press.

Gerz, T. & Schumann, U. 1990 Direct simulation of homogeneous turbulence and gravity waves in sheared an unsheared stratified flows. In: *Turbulent Shear Flow 7* (F. Durst et al., ed.), Springer-Verlag, in press.

Gerz, T., Schumann, U. & Elghobashi, S.E. 1989 Direct numerical simulation of stratified homogeneous turbulent shear flows; *J. Fluid Mech.* **200**, 563-594.

Hunt, J.C.R., Stretch, D.D. & Britter, R.E. 1988 Length scales in stably stratified turbulent flows and their use in turbulence models. In: *Stably Stratified Flows and Dense Gas Dispersion* (J.S. Puttock, ed.), Clarendon Press, Oxford, pp. 285-321.

Rogers, M.M., Mansour, N.N. & Reynolds, W.C. 1989 An algebraic model for the turbulent flux of a passive scalar. *J. Fluid Mech.* **203**, 77-101.

Tavoularis, S. & Corrsin, S. 1981 Experiments in nearly homogeneous turbulent shear flow with a uniform mean temperature gradient, Part 1. *J. Fluid Mech.* **104**, 311-347.

Tavoularis, S. & Corrsin, S. 1985 Effects of shear on the turbulent diffusivity tensor. *Int. J. Heat Mass Transfer* **28**, 265-276.

Tavoularis, S. & Karnik, U. 1989 Further experiments on the evolution of turbulent stresses and scales in uniformly sheared turbulence. *J. Fluid Mech.* **204**, 457-478.